Preprints of the 21st IFAC World Congress (Virtual)
Berlin, Germany, July 12-17, 2020

Towards observer-based tunneling current calibration in an experimental STM device.

Gildas Besançon * **Alina Voda** * **Andrei Popescu** *

* *Univ. Grenoble Alpes, CNRS, Grenoble INP* [1]
GIPSA-lab, 38000 Grenoble, France
(e-mail:{gildas.besancon, alina.voda}@grenoble-inp.fr).

Abstract: In the context of experimental modeling for a Scanning Tunneling Microscope (STM) prototype, a reduced order observer is proposed for parameter adaptation in the tunneling current model. The underlying dynamical model is first recalled, and the proposed observer is then presented, and discussed. The approach is finally illustrated with real data taken from the prototype.

Keywords: Observer, reduced order, parameter estimation, tunneling current, STM application.

1. INTRODUCTION

Nanosciences are a source of challenging problems in estimation and control (Voda, 2010; Clévy et al., 2011; Eleftheriou and Moheimani, 2011; Fleming and Leang, 2014).
In the specific area of Scanning Probe Microscopy, the so-called *Scanning Tunneling Microscope* (STM) is the one which first gave birth to the whole field, in the early eighties (Binnig and Rohrer, 1986). As meant by its name, it is based on the *tunneling current* phenomenon, and is the first instrument that allowed surface imaging at atomic resolution.
Even though now pretty well known, this approach still presents challenges in control, as addressed in (Bonnail et al., 2004) or some former studies of ours (Ahmad et al., 2008, 2012; Ryba et al., 2013) for instance, up to more recent works of (Tajaddodianfar et al., 2017, 2018). In particular, it requires specific calibrations for the device to be properly operated, and in the present paper, a simple observer approach is proposed to identify a parameter that enters into the dynamical description of tunneling effect, thus making it instrumental in the use of an STM for surface imaging (see e.g. (Besançon et al., 2016; Popescu et al., 2018)).
This work is based on an experimental device which was developed in Gipsa-lab for the purpose of such studies (Blanvillain et al., 2008, 2014).

The formal statement of the estimation problem under study is first given in section 2, together with the presentation of the underlying device. The observer solution, finally given under the form of a reduced order one, is then discussed in section 3, and related application results based on real data from our experimental device are presented in section 4. Some conclusions and considerations for future works end the paper in section 5.

[1] *Institute of Engineering Univ. Grenoble Alpes*

2. PROBLEM STATEMENT

2.1 STM device under consideration

Standard STM operation (Julian Chen, 2008) in short means approaching a tip to the surface under study, close enough (less than 1nm) so that an applied voltage between both (bias voltage) results in a (quantum) current effect, called *tunneling* current. The control task is then to regulate this distance.

In the considered Gipsa STM device (shown in figure 1), the vertical motion is driven by a piezo actuator, fed by a voltage generated numerically (via a PC) and appropriately amplified (via a Voltage Amplifier), while the obtained current is in its turn amplified and measured (via a Current Sensor), and brought back to the numerical equipment (PC).

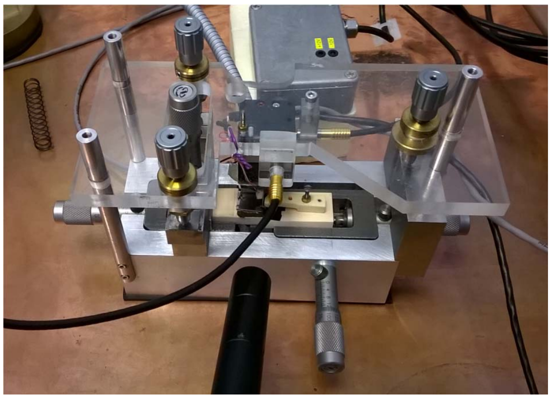

Fig. 1. STM prototype.

This operation is summarized by the schematic view of figure 2 below. Full technical details on this instrumentation can be found in (Popescu et al., 2018) for instance.

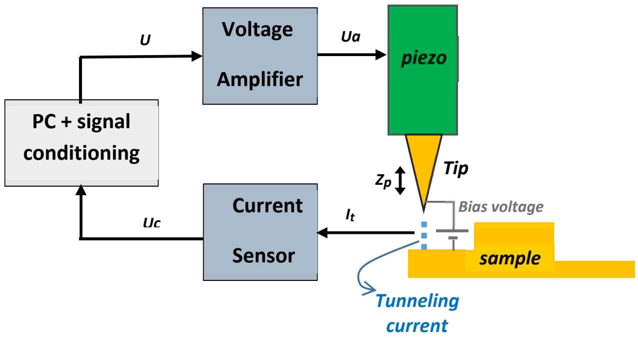

Fig. 2. STM vertical operation.

For a mathematical description of the whole dynamical behaviour, let us recall modeling basics for each element (see again figure 2 for notations).
First, the piezoactuator dynamics can typically be represented by a second order model (eg as in Ryba et al. (2013)), that is:

$$Z_p(s) = \frac{G_p w_p^2}{s^2 + 2\zeta_p w_p s + w_p^2} U_a(s) \tag{1}$$

where s stands for Laplace variable, $Z_p(s)$ and $U_a(s)$ Laplace transforms of piezo displacement and its applied (amplified) voltage, respectively, and G_p, w_p, ζ_p the piezo DC gain, natural pulsation, and damping coefficient respectively.
Similarly, the dynamics of both voltage amplifier and current sensor can be captured by simple 1st order models, that is:

$$U_a(s) = \frac{G_v w_v}{s + w_v} U(s) \text{ and } U_c(s) = \frac{G_i w_i}{s + w_i} I_t(s) \tag{2}$$

respectively, where U, U_c and I_t refer to Laplace transforms of the applied voltage, the voltage read by the current sensor and the tunneling current respectively, while G_v, G_i denote voltage and current gains respectively, and w_v, w_i the corresponding bandwidths.
In practice, the piezo actuator bandwidth in our device being about ten times larger than those of the other elements, its dynamics will be neglected in the present study. This means that piezo model (1) will be restricted to its DC gain G_p.
Finally, the tunneling current can be usually expressed according to the tip motion z_p with respect to the sample position z_s, and initial tip-sample surface d_0, as depicted by figure 3.
This results in the following expression:

$$i_t = gV_b exp(-k(d_0 + z_p - z_s)) \tag{3}$$

where g is a constant depending on the materials, V_b is the applied voltage, and k the typical exponential rate of the current variation with respect to tip-sample distance.

This means that we can finally end up with a state space representation of the following form:

$$\begin{aligned} \dot{x}_1(t) &= -w_i x_1(t) + G_i w_i g V_b exp(-k(d_0 + x_2(t) - z_s(t))) \\ \dot{x}_2(t) &= -w_v x_2(t) + G_p G_v w_v u(t) \\ y(t) &= x_1(t) \end{aligned} \tag{4}$$

where x_1 stands for u_c, x_2 for z_p and u for the applied voltage.

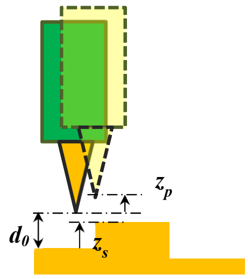

Fig. 3. Vertical Z-motion.

2.2 Estimation problem under consideration

Typically in the above model, z_s will vary in some unknown way during a scanning operation mode, and from the knowledge of everything else, its variation can be recovered, giving an image of the surface (Julian Chen, 2008).
In the present paper instead, we will focus on the characterization of the tunneling parameters, and in particular coefficient g, which may be inaccurately known in practice. This step thus comes prior to any scanning, and can be also an opportunity to calibrate the operation with respect to values of d_0 and initial sample level z_s for instance.
In other words, we consider here the problem of estimating parameter $gV_b exp(-k(d_0 + z_s))$ when z_s is supposed to be constant (no scanning). Of course if d_0 and z_s are known, then g can be obtained, and conversely, whenever gV_b is known, $z_s + d_0$ can be estimated. Notice that those parameters cannot be separately identified.

Setting $\theta := gV_b exp(-k(d_0 + z_s))$ then, we are brought to an observer problem for the following system:

$$\begin{aligned} \dot{x}_1(t) &= -w_i x_1(t) + \theta G_i w_i exp(-k x_2(t)) \\ \dot{x}_2(t) &= -w_v x_2(t) + G_p G_v w_v u(t) \\ y(t) &= x_1(t) \end{aligned} \tag{5}$$

where y denotes the available measurement, and u the known applied voltage, while θ (and state variable x_2) are to be estimated.

3. OBSERVER SOLUTION

3.1 High gain approach

It is clear that model (5) can be extended with unknown parameter θ as an additional state variable in the following way:

$$\begin{aligned} \dot{x}_1(t) &= -w_i x_1(t) + \theta G_i w_i exp(-k x_2(t)) \\ \dot{x}_2(t) &= -w_v x_2(t) + G_p G_v w_v u(t) \\ \dot{\theta} &= 0 \\ y(t) &= x_1(t) \end{aligned} \tag{6}$$

and that an observer can be built for this extended model.

So called *uniform observability* property (Gauthier and Bornard, 1981) can indeed here be checked, and a diffeomorphism can be found to turn the model into an appropriate form for a well-known *high gain observer design* (Gauthier et al., 1992):

Proposition 1. The system below:

$$\dot{\xi} = A\xi - \Lambda(\lambda)K(C\xi - y) + \varphi(\xi, u) \quad (7)$$

$$\begin{pmatrix} \hat{x}_1 \\ \hat{x}_2 \\ \hat{\theta} \end{pmatrix} = \begin{pmatrix} \xi_1 \\ \frac{\xi_3}{kw_v\xi_2} \\ \frac{\xi_2}{G_iw_i}exp(\frac{\xi_3}{w_v\xi_2}) \end{pmatrix} \quad (8)$$

with $A = \begin{pmatrix} 0 & 1 & 0 \\ 0 & 0 & 1 \\ 0 & 0 & 0 \end{pmatrix}$, $C = (1\ 0\ 0)$, $\Lambda(\lambda) = \begin{pmatrix} \lambda & 0 & 0 \\ 0 & \lambda^2 & 0 \\ 0 & 0 & \lambda^3 \end{pmatrix}$ and

$$\varphi(\xi, u) = \begin{pmatrix} -w_i\xi_1 \\ -kG_pG_vw_v\xi_2u \\ -w_v\xi_3 + kG_pG_vw_v^2\xi_2u - kG_pG_vw_v\xi_3u + \frac{\xi_3^2}{\xi_2} \end{pmatrix}$$

provides an observer for system (6), in the sense that $\hat{x}_i(t) - x_i(t)$ for $i = 1, 2$, and $\hat{\theta}(t) - \theta$, can asymptotically decay to zero for any initial condition, whenever K is chosen such that $A - KC$ is Hurwitz, φ is saturated according to some bounded domain of x_1, x_2, θ, and λ is large enough. ◇

The formal verification follows classical lines of high gain observers, and is omitted here, since it will not be the approach finally chosen.
The usual advantage indeed in such an approach is the guarantee of convergence even in the presence of nonlinearities, as well as the single tuning coefficient λ (*high gain*). But a classical counterpart is the possible amplification of the measurement noise effect (see (Astolfi et al., 2016) for instance), which is quite significant in our application, and makes this high gain technique indeed too sensitive to the noise. One could think of some possible improvements (e.g. as in (Ahrens and Khalil, 2009; Boizot et al., 2009), but we instead propose here to consider a more simple approach, presented in next section.

3.2 Reduced order approach

As an alternative approach, owing to the property that trajectories in x_2 all converge to each other, we can propose a more simple *reduced order* observer (*e.g.* in the spirit of Besançon (2000)) as follows:

Proposition 2. For system (5) with u such that x_1 and x_2 remain within positive bounded intervals, the system below provides asymptotic estimates $\hat{x}_2$ and $\hat{\theta}$ for x_2 and θ respectively, for any $\gamma > 0$:

$$\begin{aligned} \dot{\hat{x}}_2(t) &= -w_v\hat{x}_2(t) + G_pG_vw_vu(t) \\ \dot{\hat{\zeta}}(t) &= -\gamma G_iw_iexp(-k\hat{x}_2(t))[\hat{\zeta}(t) + \gamma y(t)] + \gamma w_iy(t) \\ \hat{\theta}(t) &= \hat{\zeta}(t) + \gamma y(t) \end{aligned} \quad (9)$$

Proof. The verification goes as follows: first set $\zeta := \theta - \gamma x_1$ and notice that the parameter estimation error $\hat{\theta} - \theta$ then coincides with $e_\zeta := \hat{\zeta} - \zeta$. This means that we are brought to the study of the latter.
Then, one can check that:

$$\begin{aligned} \dot{e}_\zeta &= -\gamma G_iw_iexp(-kx_2)e_\zeta \\ &\quad -\gamma G_iw_i[exp(-k\hat{x}_2) - exp(-kx_2)] \times [\hat{\zeta} + \gamma y] \\ &=: -\gamma G_iw_iexp(-kx_2)e_\zeta + \delta \end{aligned} \quad (10)$$

where δ depends on the difference between $\hat{x}_2$ and x_2, as well as $\hat{\zeta}$ and y.
It is clear, from the system and observer equations, that $e_2 := \hat{x}_2 - x_2$ satisfies:

$$\dot{e}_2 = -w_ve_2$$

meaning that $\hat{x}_2$ exponentially approaches x_2.
In addition, from equations (9) and boundness of y, it results that $\hat{\zeta}$ is also bounded.
This means that δ is exponentially vanishing.

Now since x_2 remains bounded, e_ζ is clearly ISS w.r.t. δ, and since δ goes to zero, so does e_ζ (in addition, it is also clear that one can tune the rate of decay via the choice of parameter γ). ◀

Beyond its simplicity (second order only, and still with a single tuning parameter, γ), this approach also ensures some properties with respect to the noise effect (similarly to the adaptive observer approach of Zhang (2002) for instance): in short, the error is guaranteed to converge in mean value, and the tuning parameter γ can even be chosen according to a filtering purpose.
If indeed the measurement takes the form:

$$y = x_1 + \nu \quad (11)$$

where ν stands for some measurement noise assumed to be a gaussian white noise, the estimation error e_ζ with the above notations, now satisfies:

$$\begin{aligned} \dot{e}_\zeta &= -\gamma G_iw_iexp(-kx_2)e_\zeta - \gamma^2G_iw_iexp(-k\hat{x}_2)\nu + \gamma w_i\nu \\ &\quad -\gamma G_iw_i[exp(-k\hat{x}_2) - exp(-kx_2)] \times [\hat{\zeta} + \gamma x_1 + \gamma\nu] \\ &=: -\gamma G_iw_iexp(-kx_2)e_\zeta - \gamma^2G_iw_iexp(-k\hat{x}_2)\nu + \gamma w_i\nu \\ &\quad +\delta_1 \end{aligned} \quad (12)$$

where δ_1 is still vanishing.
It is here clear that x_2 and $\hat{x}_2$ are independent of ν, so that the mean value of e_ζ satisfies:

$$\frac{d\bar{e}_\zeta}{dt} = -\gamma G_iw_iexp(-kx_2)\bar{e}_\zeta + \bar{\delta}_1 \quad (13)$$

where $\bar{\cdot}$ refers to the mean.
From this, and the fact that δ_1 vanishes, we get that $\bar{e}_\zeta$ also asymptotically decays to zero.

In a similar way, it can be checked that the variance of e_ζ asymptotically behaves as the solution Q of:

$$\dot{Q} = -2\gamma G_iw_iexp(-kx_2)Q + \gamma^2w_i^2(\gamma G_iexp(-k\hat{x}_2) + 1)^2V \quad (14)$$

where V stands for the noise intensity.
From this, the smaller γ is, the smaller this variance is in turn.

4. ESTIMATION RESULTS WITH REAL DATA

The above approach has been tested with data recorded from our Gipsa-lab STM prototype (Blanvillain et al., 2014) (see tip picture in fig. 4 hereafter).

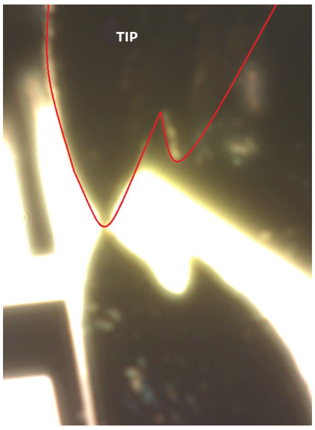

Fig. 4. Real tip and its reflection.

The corresponding numerical values for model (5) are summarized in table 1 below.

G_v	$15\,V/V$
f_v	$4\,kHz$
G_i	$1e9\,V/A$
f_i	$13\,kHz$
k	$16.5nm^{-1}$
G_p	$1.2\,nm/V$

Table 1. Numerical data

For this system, measurements are obtained when operating the STM in a fixed position, under simple PI regulation of the distance between tip and sample (via output direct regulation).

The corresponding output measurement and available control input are presented in figures 5 and 6 respectively, over 5 seconds (under a setpoint control during 3 seconds first, then followed by a square wave tracking configuration).

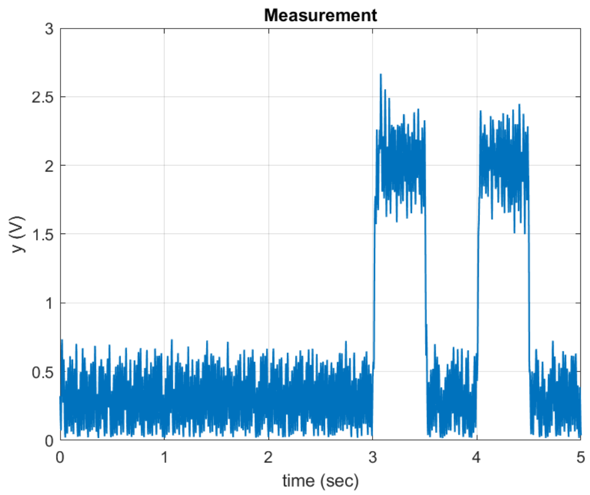

Fig. 5. Measured output (as delivered by current sensor, under closed loop operation).

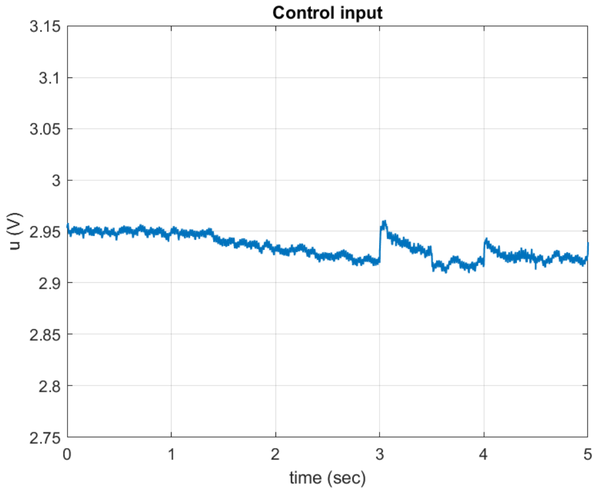

Fig. 6. Control input (as fed to the voltage amplifier, during closed loop operation).

The estimation for coefficient gV_b with the above reduced order observer is then tested with those data, and considering some rough estimate for $d_0 + z_s$ here set to $52.13\,nm$.

Noting yet, from the control profile, that after about 1.5 second, a drift-like disturbance appears (as often with piezoactuation in such devices (Rakotondrabe et al., 2010)), the estimation of gV_b is here considered on earlier times only, say up to time 1.4 second. This means that the convergence should be fast enough (γ large enough), but with enough noise attenuation (γ not too large).

A first estimation result is displayed on fig. 7, obtained with $\gamma = 1e10$: the convergence can be seen to be here very fast (notice that the parameter estimate is initialized at 0), but the estimate is very *noisy* (it seems to reach a value of about $1e-3$, but with variations up to 7 times this value).

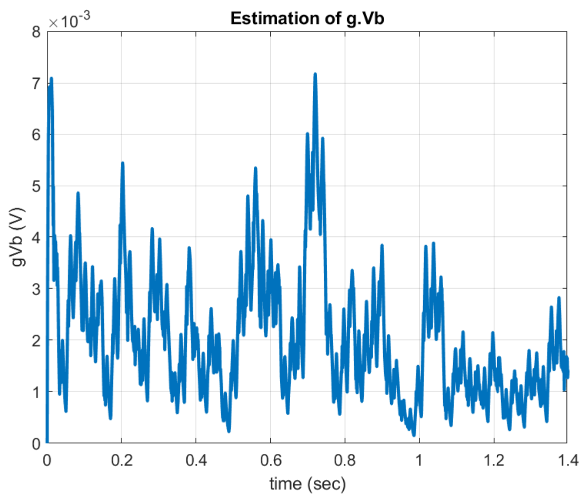

Fig. 7. Estimation result for gV_b with $\gamma = 1e10$.

A second result with a lower γ $(1e8)$ is then presented in figure 8, illustrating the noise effect reduction (as expected from the discussion after proposition 2), and emphasizing a final value around 0.0011. This is confirmed by the superposed result of an additionally filtered version of this estimate, displayed in dahsed line on the same figure (just using a low-pass filter).

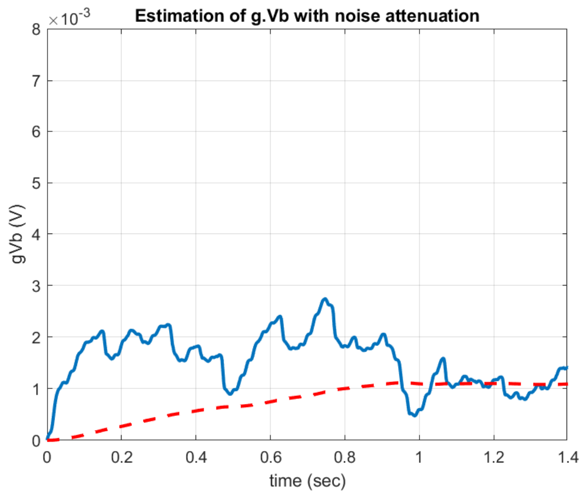

Fig. 8. Estimation result for gV_b with $\gamma = 1e8$ (and filtered version in dashed red line).

Notice then that the estimate of gV_b can be frozen after time $t = 1.4$ second for instance, and going on with the same observer allows now to estimate the *drift*, in terms of tip-sample distance.
The corresponding estimation result is shown in figure 9.

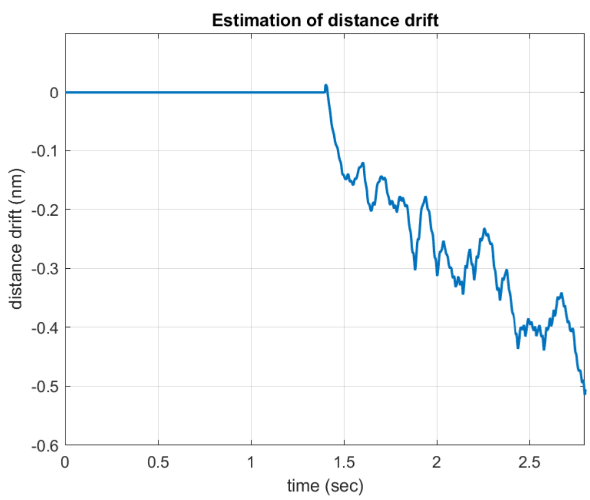

Fig. 9. Estimation result for distance drift, started after time $1.4\,sec$ (and based on the estimate for gV_b obtained before time $1.4\,sec$).

Notice finally that combining this drift estimate with the frozen estimate of gVb and that of x_2, the actual tunneling current can be estimated in its turn, and the corresponding result is presented in figure 10. An additionally filtered estimate is displayed as well, emphasizing the current regulation around a value of about $0.3nA$.
From the estimated gV_b and the available output measurement, this means a distance of about $0.92\,nm$.

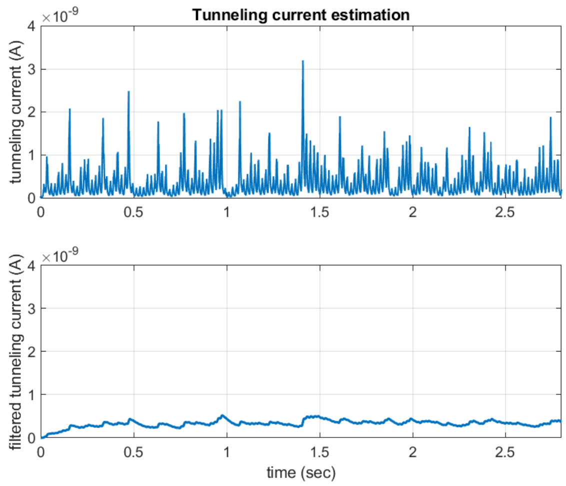

Fig. 10. Tunneling current estimate (reconstructed from gV_b and drift estimates) - top: direct estimate, bottom: filtered estimate.

5. CONCLUSIONS

In this paper an observer approach has been discussed for a problem of parameter estimation in tunneling current modeling. The approach has been formally presented, and illsutrated on the basis of real data taken from a prototype experiment. The focus has been made on a single parameter (or combination of parameters), which can be either related to tunneling current characteristics, or to tip-sample distance.
The extension to the full parametric characterization of the tunneling current will be part of future developments, as well as its possible use in control and imaging purposes.

ACKNOWLEDGEMENTS

This work has been partly supported by the LabEx PERSYVAL-Lab (ANR-11-LABX-0025-01) funded by the French program Investissement d'avenir.

REFERENCES

Ahmad, I., Voda, A., Besançon, G., and Buche, G. (2012). Robust digital control approach for high performance tunneling current measurement system. *Control Engineering Practice*, 20(7), 643–653.

Ahmad, I., Voda, A., and Besançon, G. (2008). Controller design for a closed-loop scanning tunneling microscope. In *4th Annual IEEE Conference on Automation Science and Engineering, Washington DC, USA*.

Ahrens, H. and Khalil, H. (2009). High-gain observers in the presence of measurement noise: A switched-gain approach. *Automatica*, 45(4), 936–43.

Astolfi, D., Marconi, L., Praly, L., and Teel, A. (2016). Sensitivity to high-frequency measurement noise of nonlinear high-gain observers. In *10th IFAC Symposium on Nonlinear Control Systems, Monterey, CA, USA*.

Besançon, G. (2000). Remarks on nonlinear adaptive observer design. *Systems & Control Letters*, 41, 271–280.

Besançon, G., Ryba, L., Popescu, A., Voda, A., and Stefanoiu, D. (2016). Experimental nanosurface imaging with a scanning-tunneling-like device under 3D control. In *Proc. 20th International Conference on System Theory, Control and Computing, Sinaia, Romania*.

Binnig, G. and Rohrer, H. (1986). Scanning tunneling microscopy. *IBM Journal of Research and Development*, 30, 355–369.

Blanvillain, S., Voda, A., and Besançon, G. (2008). Pull-in control during nanometric positioning by near field position sensing. In *47th IEEE Conference on Decision and Control (CDC 2008)*, 5194–5199.

Blanvillain, S., Voda, A., Besançon, G., and Buche, G. (2014). Subnanometer positioning and drift compensation with tunneling current. *IEEE Transactions on Control Systems Technology*, 22(1), 180–189.

Boizot, N., Busvelle, E., and Gauthier, J.P. (2009). An adaptive high-gain observer for nonlinear systems. *Automatica*, 46(9), 1483–88.

Bonnail, N., Tonneau, D., Jandard, F., Capolino, G.A., and Dallaporta, H. (2004). Variable structure control of a piezoelectric actuator for a scanning tunneling microscope. *IEEE Trans. Industrial Electronics*, 51.

Clévy, C., Rakotondrabe, M., and Chaillet, N. (eds.) (2011). *Signal Measurement and Estimation Techniques for Micro and Nanotechnology*. Springer.

Eleftheriou, E. and Moheimani, S. (2011). *Control Techno. for Emerging Micro & Nanoscale Systems*. Springer.

Fleming, A.J. and Leang, K.K. (2014). *Design, Modeling and Control of Nanopositioning Systems*. Springer.

Gauthier, J.P., Hammouri, H., and Othman, S. (1992). A simple observer for nonlinear systems-applications to bioreactors. *IEEE Transactions on Automatic Control*, 37(6), 875–880.

Gauthier, J. and Bornard, G. (1981). Observability for any $u(t)$ of a class of nonlinear systems. *IEEE Transactions on Automatic Control*, 26(4), 922–926.

Julian Chen, C. (2008). *Introduction to Scanning Tunneling Microscopy*. Oxford Science Pub.

Popescu, A., Besançon, G., Voda, A., and Basrour, S. (2018). Control-observer technique for surface imaging with an experimental platform of scanning-tunneling-microscope type. In *Proc. American Control Conference, Milwaukee, USA*.

Rakotondrabe, M., Clevy, C., and Lutz, P. (2010). Complete open loop control of hysteretic, creeped, and oscillating piezoelectric cantilevers. *IEEE Transactions on Automation Science and Engineering*, 7(3), 440–450.

Ryba, L., Voda, A., and Besançon, G. (2013). Modelling and control of 3d stm-like scanning device with application to surface reconstruction. In *Methods and Models in Automation and Robotics (MMAR), 2013 18th International Conference on*, 479–484.

Tajaddodianfar, F., Moheimani, S.O.R., Fuchs, E., and Randall, J.N. (2017). Stability analysis of a scanning tunneling microscope control system. In *Proc. American Control Conference, Seattle, USA*.

Tajaddodianfar, F., Moheimani, S.O.R., Owen, J., and Randall, J.N. (2018). On the effect of local barrier height in scanning tunneling microscopy: Measurement methods and control implications. *Review of Scientific Instruments*, 89.

Voda, A. (ed.) (2010). *Micro, Nanosystems and systems on chips – modelling, control and estimation*. Wiley.

Zhang, Q. (2002). Adaptive observer for mimo linear time varying systems. *IEEE Trans Automatic Control*, 47, 525–529.